J Neuroimmune Pharmacol (2011) 6:640–649
DOI 10.1007/s11481-011-9289-0

ORIGINAL ARTICLE

A Failure to Normalize Biochemical and Metabolic Insults During Morphine Withdrawal Disrupts Synaptic Repair in Mice Transgenic for HIV-gp120

Veera Venkata Ratnam Bandaru · Neha Patel · Ostefame Ewaleifoh · Norman J. Haughey

Received: 1 March 2011 / Accepted: 26 June 2011 / Published online: 12 July 2011

Abstract Drug abuse in HIV-infected individuals accelerates the onset and progression of HIV-associated neurocognitive disorders (HAND). Opiates are a class of commonly abused drugs that have interactive effects with neurotoxic HIV proteins that facilitate glial dysfunction, neuronal damage and death. While the combined effects of neurotoxic HIV proteins and morphine have been extensively studied in the setting of chronic and acute morphine use, very little in known about the effects of HIV proteins during drug withdrawal. Since opiate withdrawal can induce considerable neuronal stress, we determined the effects of opiates (morphine) on brain redox balance, sphingolipid metabolism and synaptic integrity during both chronic and withdrawal conditions in non-transgenic mice (nTg), and in mice transgenic for the HIV-coat protein gp120 (gp120tg). In nTg mice, we found that chronic morphine increased brain oxidative capacity and induced synaptic damage that was largely reversed during drug withdrawal. Gp120tg mice showed a similar response to chronic morphine, but the diminished oxidative capacity and synaptic damage failed to normalize during drug withdrawal. In nTg mice, brain sphingolipid content was not affected by morphine during chronic or withdrawal conditions. In gp120tg mice there was a baseline perturbation in sphingolipid metabolism that manifest as decreased sphingomyelin with accumulations of the bioactive lipid ceramide. Sphingolipid metabolism was highly reactive to morphine in gp120tg mice. Chronic morphine increased sphingomyelin content with a consequent reduction in ceramide. During drug withdrawal, these effects reversed, and sphingomyelin levels were reduced with consequent increases of ceramide. We interpret these findings to suggest that neuronal repair during morphine withdrawal is inhibited in the setting of gp120 by mechanisms that involve sustained oxidative insult and accumulations of the highly reactive intermediate ceramide.

Keywords HIV · HAND · Morphine · Opiates · Neuron · Withdrawal · Oxidative stress · Sphingomyelin · Ceramide · Synapse · PSD95

V. V. R. Bandaru · N. Patel · O. Ewaleifoh · N. J. Haughey (✉)
Department of Neurology, Division of Neuroimmunology,
Johns Hopkins University School of Medicine,
Meyer 6-109, 600 North Wolfe Street,
Baltimore, MD 21287, USA
e-mail: nhaughe1@jhmi.edu

Introduction

HIV-infected people who also abuse opiates often show faster rates of disease progression including early and rapidly progressing HIV-Associated Neurocognitive Disorders (HAND). Heroin undergoes first pass metabolism in liver to be converted to morphine, making morphine the most commonly used agent to study opiate effects in both in vitro and in vivo neurological systems. Nontoxic concentrations of morphine have a variety of effects on CNS function that include alterations in cytokine balance, blood brain barrier (BBB) permeability and synaptic simplification. Morphine increases inflammatory cytokine release from glia with consequent reductions in the expression of several tight junctional proteins including ZO-1, Jam-2, occludin and P-glycoprotein expression. These perturbations increase the endothelial adhesion of monocytes and the transendothelial migration of these cells across the BBB where they can modify the biochemical environment in brain parenchyma (Mahajan et al. 2008; Stefano et al. 1998a, b). Morphine also has direct effects on brain resident cells and directly interacts with astrocytes to increase their activation state, and decreases expression of the protective cytokines IL-8 and MIP-β

(Mahajan et al. 2002; Bruce-Keller et al. 2008). Although morphine appears to not induce a generalized death of neurons, there is evidence that morphine induces the death of GABAergic interneurons, induces a neuronal stress response in cortical and striatal neurons and reduces spine density (Sultana et al. 2010; Fitting et al. 2010).

In addition to direct effects on brain resident cells, morphine potentiates the glial response to a variety of stimuli including HIV-proteins (Hauser et al. 2000; Gurwell et al. 2001). For example, morphine in combination with the HIV trans-acting protein Tat perturbs proteosome activity, induces the generation of reactive oxygen species (ROS), increases protein oxidation and increases expression of the pro-inflammatory cytokines MCP-1, RANTES and IL-6, although a reduced expression of TNFα, IL-6 and MCP-1 has also been reported in microglia stimulated with Tat and morphine (El-Hage et al. 2005; Turchan-Cholewo et al. 2009). The combined effects of morphine and Tat induces death of select populations of astrocytes, reduces the survival of glial progenitors, and induces a phenotype consistent with activation of apoptotic pathways in oligodendrocytes (Khurdayan et al. 2004; Hauser et al. 2009). Likewise, morphine has been shown to enhance neuronal death induced by the HIV-1 Tat protein (Gurwell et al. 2001). Less is known about the potential interactive effects of morphine with the HIV-coat protein gp120. HIV-gp120 may enhance the effects of opiates by up-regulating mu opioid receptors on macrophages and glia through autocrine/paracrine actions that involve TNF-α (Beltran et al. 2006; Chang et al. 2007). Morphine has also been shown to enhance the cytotoxicity of gp120 through p38 mitogen-activated protein kinase signaling, and by increasing the expression of CCR5 and altering the function of CXCR4 (Mahajan et al. 2002, 2008; Pitcher et al. 2010; Hu et al. 2005).

Since opiate abuse often involves cycles of intoxication followed by withdrawal, the effects of morphine withdrawal are likely to contribute to neuronal damage in HIV-infected individuals. However, the vast majority of research published to date has used combinations of HIV proteins and morphine to study interactive effects that occur during acute or chronic morphine exposure. Withdrawal from morphine is accompanyed by increased neuronal sensitivity to stress, suggesting that neurons would be highly sensitized to the toxic effects of HIV proteins during drug withdrawal. Consistent with this notion, morphine withdrawal has been shown to sensitize rodents to LPS-induced lethality by increasing the production of TNF-α, and by priming proapoptotic pathways in cortex and hippocampus that include Fas, Bad, caspases-8 and −3 signaling (Emeterio et al. 2006). In neurons, withdrawal from morphine increases the phosphorylation of NMDA receptor subunits NR1 and NR2B, and induces activation of ERK1/2, calmodulin-dependent kinase II, and cAMP response element binding proteins (Liu et al. 2010), demonstrating that neuronal signaling can be dramatically modified during morphine withdrawal. In this study we sought to determine the interactive effects of the HIV-1 protein gp120, morphine intoxication and drug withdrawal on neuronal stress and synaptic integrity in vivo, using mice transgenic for the HIV-coat protein gp120.

Methods

Animals and experimental treatments Six month old C57BL-6 non-transgenic (nTg) mice, and C57BL-6 mice transgenic for gp120 (gp120tg) were used in these studies. Gp120 mice were obtained from Dr. Lennart Muke (Gladstone Institute) and express a GFAP promoter driven HIV-1 env gene (HIV-1_{LAV}: Toggas et al. 1994). Morphine was administered by subcutaneous implantation of time-release 25 mg pellets (NIDA, Rockville, MD). These pellets deliver 5 mg/day morphine for up to 5 days (Bruce-Keller et al. 2008). Mice were sacrificed at 4 days post-implant for studies of morphine intoxication and at 7-days post-implant for studies on drug withdrawal. A total of 6 mice for each experimental group were used for these studies. Brains were rapidly removed and snap-frozen for biochemical and protein studies.

Fluorometric enzymatic assays A Cobas Fara II centrifugal fluorometric-analyzer (Roche Diagnostics, Montclair, NJ) was used to detect and quantify the presence of catalase, super oxide dismutase (SOD), glutathione and uric acid.

Glutathione The glutathione assay (OXIS Research, Portland Oregon) measures the amount of endogenous glutathione using a single substitution reaction in which the thiol group of glutathione in the sample replaces a halogen on R2 (4-clorolo-1 –methyl- 7- tri fluromethyl-quinolinium methylsulfate) forming a thioether. Under alkaline conditions (pH >13.4), R3 then transforms the substitution product (thioester) into a chromophoric thione. The thione formed has maximal absorbance at 400 nm. The amount of endogenous oxidized glutathione (GSSG) was detected using the enzyme glutathione reductase, and the cofactor NADPH. This assay introduces a radical scavenger M2VP (1-Methyl −2- thioethyl 2-pyidinium) salt that stabilizes GSH in the sample, ensuring that it is not detected as interference when GSSG is measured. To accomplish this, M2VP forms a stable UN reacting compound with endogenous GSH leaving only GSSG in the sample. Meta-phosphoric acid (5%) was added to the mixture and a 20 fold dilution of sample was made using the GSSG buffer. Glutathione reductase enzyme and NADPH were mixed in a 1:1:1:1:1 ratio. In this step the endogenous GSSG

is converted back to GSH and detected at 412 nm as NADPH that is oxidized to NADP.

Super oxide dismutase The SOD assay (Fluka, Switzerland) catalyzes the dismutation of super oxide anions into hydrogen peroxide and elemental oxygen. In this reaction, super oxide anions are produced by the action of xanthine oxidase that converts xanthine to uric acid. Xanthine oxidase also converts the tetrazolium salt (2-4-Iodophenyl-3-4-Nitrophenyl-5-2, 4 –disulfophenyl-2H- Tetrazolium salt) to a water soluble fomazan dye which absorbs light at 550 nm.

Uric acid This assay uses uricase to produce hydrogen peroxide from uric acid (Equal Diagnostics Limited, Charlottetown, Canada). The hydrogen peroxide is then converted to a phenolic compound derivative-quinoneimine, by reacting with (4-dicholoro-2-hydroxy benzene as catalyzed by peroxidase. The red colored quinoneimine dye has a maximum absorbance at 520 nm.

Catalase The catalase assay system (Sigma, USA) is based on the ability of hydrogen peroxide to oxidize an azo chromogen with an accompanying increase in the absorbance to 410–420 nm. In the presence of catalase, the amount of hydrogen peroxide is reduced, thus inhibiting the oxidation of the azo chromogen. This inhibition of chromogen oxidation is thus proportional to the activity of catalase present in the sample.

Total oxidation In the total oxidation assay (Applied bioanalytical labs, Sarasota, FL), antioxidants in the sample suppress the oxidation of ABTS (2,2′-azino-di-[3-ethylbenzthiazoline sulphonate]) to ABTS+ by metmyoglobin. The amount of ABTS+ is measured by reading absorbance at 405 nm. The assay relies on the ability of antioxidants in the sample to inhibit the oxidation of ABTS (2,2′-azino-di-[3-ethylbenzthiazoline sulphonate]) to ABTS+ by metmyoglobin. Antioxidants present in the sample suppress the absorbance to a degree proportional to their concentration. Thus, more antioxidant activity results in less fluorescence.

Immunoblotting Western blots were conducted using published procedures (Tabatadze et al. 2010). Hippocampal tissues were homogenized in ice-cold buffer containing 20 mM Tris-HCl (pH 7.4), 50 mM NaF, 0.32 M sucrose, 2 mM EDTA, 2 mM EGTA, 0.2 mM sodium orthovanadate, 1 mM PMSF and protein inhibitor cocktail (Roche diagnostics GmbH, Germany). Proteins (10 μg of total protein per lane) were separated by sodium dodecyl sulfate-polyacrylamide gel electrophoresis and transferred to nitrocellulose membranes. Membranes were blocked in Tris-buffered saline (TBS) containing 10 mM Tris-HCl [pH 7.4], 150 mM NaCl and 0.1% Tween 20 (TBS-T) for 1 h and incubated with a antibodies to the post synaptic density-95 protein (PSD95, 1:5000, Oncogene, Cambridge, MA) and β-actin (1:1000, Sigma, St. Louis, MO) overnight at 4°C. Following incubations with primary antibodies, membranes were washed in TBS and TBS-T and incubated at room temperature for 1 h with HRP-conjugated secondary antibodies (1:5000, Goat anti-mouse IgG; 1:5000, Goat anti-rabbit IgG, Promega, WI). Immunoreactivity was visualized using Pico West SuperSignal (Pierce, Rockford, IL). Optical densities were quantified using NIH ImageJ software.

Mass spectrometric measurement of sphingolipids Crude total lipid content was extracted from brain tissues using a modified Bligh and Dyer procedure (Bandaru et al. 2007). Each sample tissue sample was weighed and homogenized at room temperature in deionized water (10 volumes to weight). Lipid content was extracted by the addition of methanol containing 53 mM ammonium formate (3 volumes) with 17 ng/ml C12:0 ceramide and C12:0 sphingomyelin as internal standards, and vortexed followed by chloroform (4 volumes). The mixture was vortexed and centrifuged at 1,000 *g* for 10 min. The chloroform was removed and dried in a vacuum dryer, and stored at −80°C. The sample was resuspended in 100% methanol for analysis by LC/MS/MS. All extractions were performed using borosilicate-coated glass tubes, pipettes, and injectors to reduce the potential loss of lipids through interactions with plastic.

ESI/MS/MS analyses were performed using methods similar to those used in previous studies (Haughey et al. 2004; Bandaru et al. 2007). Individual molecular species of sphingomyelin and ceramide (C12:0 and C16:0-C26:1), were detected and quantified by LC/MS/MS using multiple reaction monitoring (MRM). The procedure is based on high performance liquid chromatography (HPLC) for temporal resolution of compounds, with subsequent introduction into the mass spectrometer for detection and quantification by mass/charge. Samples were injected using a PAL autosampler into a PerkElmer HPLC equipped with a 2.6 μm, C18, 100 Å 50×2.1 mm column for ceramides and a 5 μm, C18, 100 Å 100×2 mm column for sphingomyelins (Phenomenex, Torrance, CA). The sample was eluted at 0.4 mL min^{-1} for ceramides and 1 ml min^{-1} for sphingomyelins. The LC column was first pre-equilibrated for 0.5 min with the first mobile phase consisting of 85% methanol, 15% H_20, and 5 mM ammonium formate. The column was then eluted with the second mobile phase consisting of 99% methanol, 1% formic acid, and 5 mM ammonium formate. The eluted sample was injected into the ion source, and the detection, and quantitation of each analyte is carried out by ESI/MS/MS in MRM mode monitoring the parent compound and products by ion scan.

Method development for the quantitative detection of each analyte was accomplished with the aid of reference standards for sphingomyelins and ceramides from Avanti Polar Lipids (Alabaster, AL). Slight differences in extraction or mass spectrometer efficiencies were normalized using internal standards (ceramide C12:0 and sphingomylein C12:0) with molecular structures similar to the analytes but not found in mammals. Area under the curve for each analyte was defined individually using the Analyst 1.4.2 software package.

Results

Mice transgenic for gp120 fail to normalize oxidative capacity during morphine withdrawal

Gp120 protein expression was detected in gp120tg mice and not in nTg mice (Fig. 1a). Morphine or placebo tablets were transplanted subcutaneously into 6-month old non-transgenic (nTg) and gp120-transgenic (gp120tg) mice, and rodents were sacrificed on days 4 and 7 post-implant. These time points were chosen to mimic chronic and drug withdrawal conditions. On day 4 post-implant, morphine levels in plasma were 2.7–3.2 ng/ml and were not different in nTg compared with gp120tg mice. Morphine was undetectable 7 days post-implant, and was not detected in animals administered placebo (Fig. 1b, c). A series of antioxidant and pro-oxidant measures were used to determine redox capacity in these rodents. Non-transgenic (nTg) and gp120 transgenic (gp120tg) mice administered placebos had a similar total oxidation capacity, superoxide dismutase (SOD) activity, uric acid levels and ratios of reduced glutathione (GSH) to oxidized glutathione (Fig. 2a–d). After 4 days of morphine there was a 24.5±5% decrease in the oxidation capacity of nTg mice, and a 41.4±4% decrease in gp120tg mice (Fig. 2a). SOD activity decreased by 19.8±6% in nTg mice, and by 21.8±3% in gp120tg mice (Fig. 2b). Uric acid levels decreased by 10.0±4% nTg, and by 16.2±3% gp120tg mice (Fig. 2c). The ratio of GSH to GSSG decreased by 46.8±12% in nTg mice and by 55.9±5% in gp120tg mice following 4 days of morphine exposure (Fig. 2d). These data show that there were no significant baseline differences in the antioxidant capacities of gp120tg compared with nTg mice, and that morphine increased oxidative stress to a similar extent in nTg and gp120tg mice.

During morphine withdrawal in nTg mice, total antioxidant capacity, SOD activity, uric acid levels, but not the GSH/GSSG ratio normalized (Fig. 2e–h). However, in gp120tg mice, the total antioxidant capacity, SOD activity, and the GSH/GSSG ratio did not recover during morphine withdrawal (Fig. 2e, f, h). Uric acid levels did normalize in gp120tg mice (Fig. 2g). These data demonstrate that morphine reduced endogenous antioxidant defenses, with a consequent accumulation of free radicals. During morphine withdrawal, oxidative balance largely normalized in nTg mice, but failed to normalize in gp120tg mice.

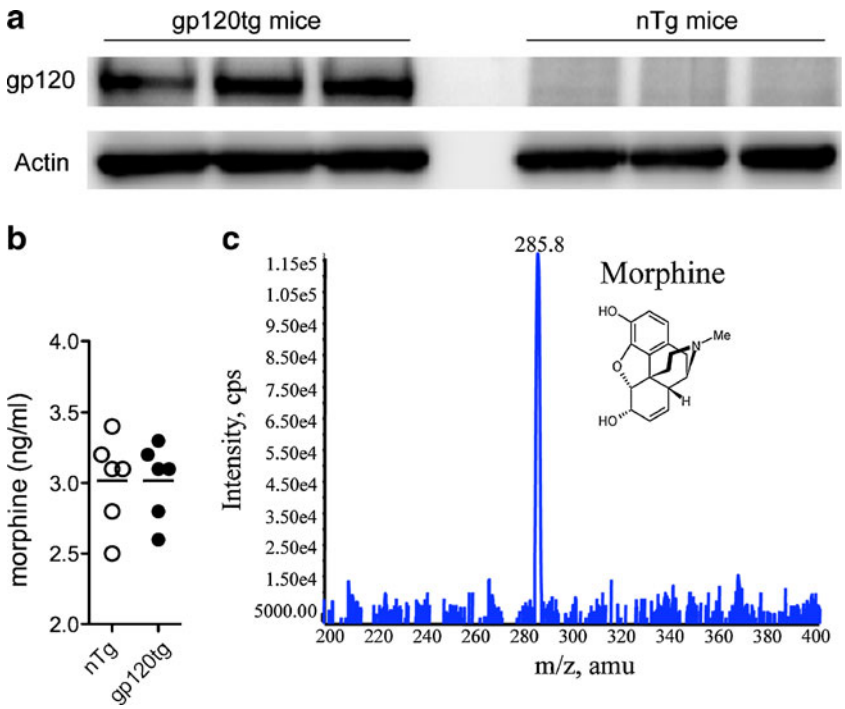

Fig. 1 Gp120 protein expression and plasma morphine levels. **a** Gp120 protein expression was detected in cortex of gp120tg mice, and was undetectable in nTg mice. Morphine levels were measured in plasma 4 days after subcutaneous implantation of time-release 25 mg pellets. **b** Scatter plot showing that morphine levels were similar in nTg and gp120tg mice 4 days after implantation of morphine pellets. **c** Mass spectra showing the detection and morphine and the corresponding molecular structure

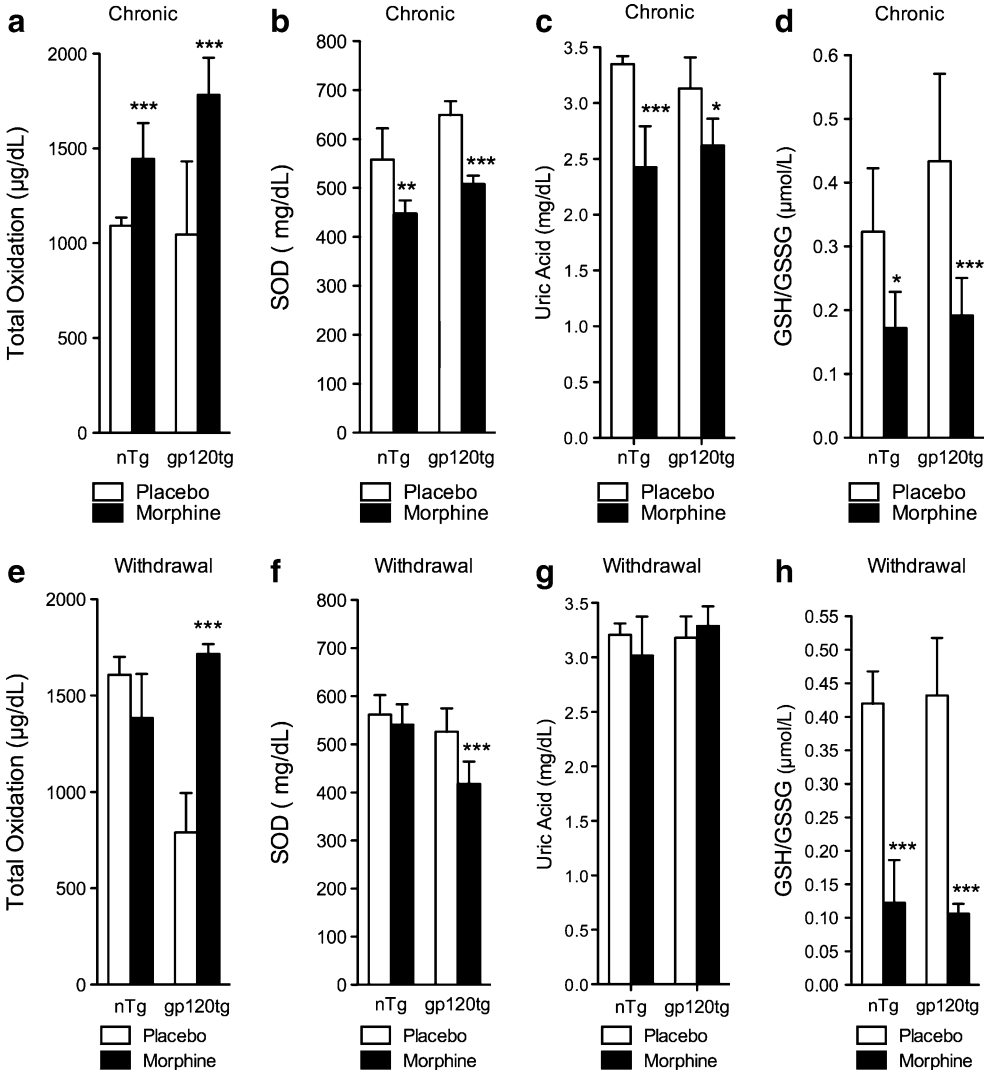

Fig. 2 Mice transgenic for HIV gp120 fail to normalize morphine-induced increases of reactive oxygen species in brain during drug withdrawal. **a–d** Chronic morphine administration increased total oxidation, and decreased SOD activity, uric acid levels and the GSH/GSSH ratio in both nTg and gp120tg mice. **e–f** During drug withdrawal, total oxidation and SOD activity normalized in nTg mice, but not in gp120tg mice. Uric acid levels normalized and the GSH/GSSG ratio failed to normalize in both groups of mice. ANOVA with Tukey post hoc comparisons (n=6 per group). *p<0.05, **p<0.01, ***p<0.001 compared with placebo

Morphine induced accumulations of sphingomyelin are metabolized to ceramide during drug withdrawal in mice transgenic for gp120

There were baseline differences in sphingomyelin and ceramide balance in gp120tg compared with nTg mice. In mice administered placebo, all sphingomyelin species measured (C16:0-C26:0) were decreased, and all (C18:0-C24:0) but one (C16:0) ceramide species were increased in gp120tg compared with nTg mice (Fig. 3a–b). These data are consistent with previous reports that accumulations of ceramide are induced by gp120 application onto cultured neurons (Haughey et al. 2004; Jana and Pahan 2004). We next determined sphingolipid and sterol levels in brains of nTg and gp120tg mice during chromic morphine administration and during morphine withdrawal. During chronic morphine administration, levels of all sphingomyelin and ceramide species were unchanged in nTg mice compared with placebo (Fig. 3a–b). In gp120tg mice, chronic morphine administration resulted in increases of multiple sphingomyelin species (C16:0-C22:1, C26:1) and decreases in several long chain ceramides (C16:0-C20:0) (Fig. 3a–b). During morphine withdrawal in gp120tg mice, sphingomyelin levels either normalized (C16:0-C22:0) or decreased (C24:0-C26:0) (Fig. 3c) and levels of all ceramides measured were increased (C16:0-C24:0) (Fig. 3d) compared to gp120tg mice administered placebo. These data demonstrate that sphingolipid metabolism is perturbed in gp120tg mice, and these pathways are sensitive to the effects of chronic morphine and drug withdrawal.

Evidence for synaptic damage in gp120 mice administered morphine

Sphingolipids are highly enriched in brain and play complex roles in regulating neuronal excitability. The sphingolipids, sphingomyelin, ceramide and sphingosine are regulators of synaptic functions, and have been shown to play important roles in synapse formation, neurotransmitter release and synaptic plasticity (Wheeler et al. 2009;

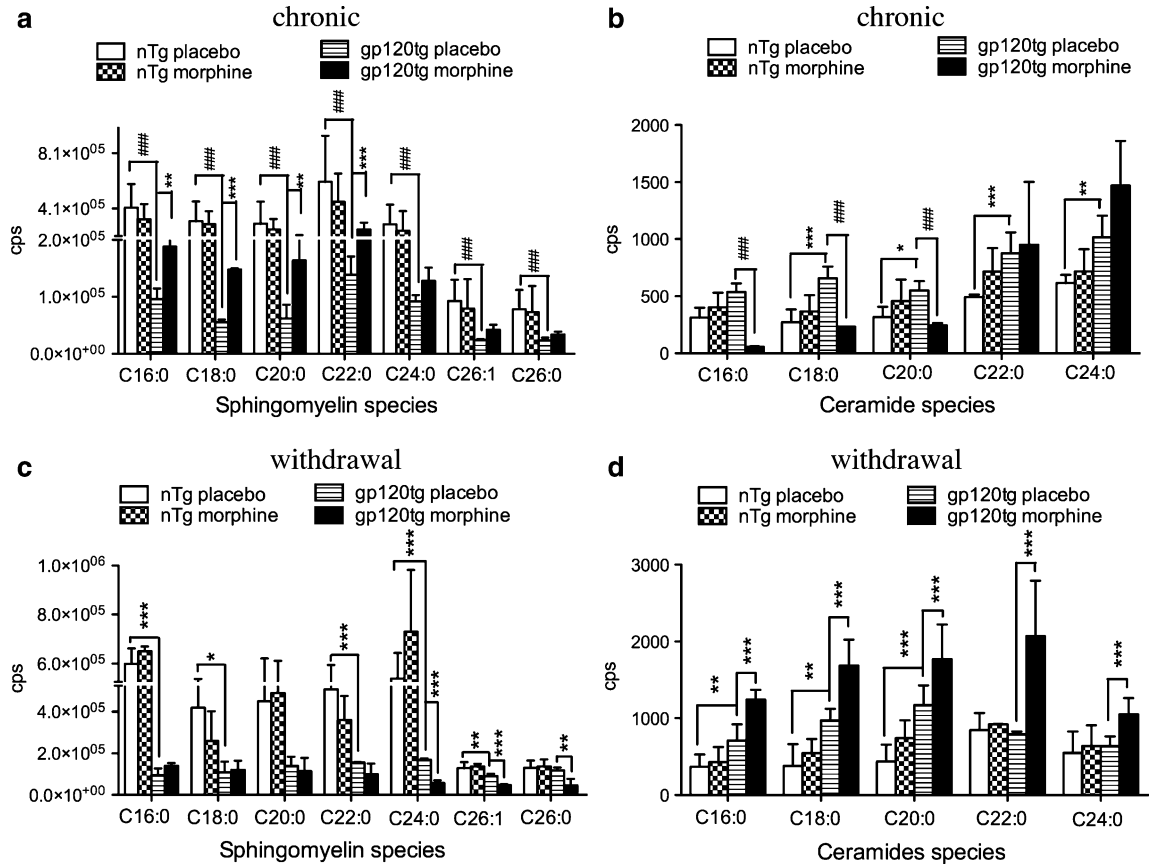

Fig. 3 Evidence that morphine induces sphingomyelin synthesis during chronic administration and sphingomyelin catabolism during drug withdrawal in brains of gp120tg mice. **a–b** Baseline levels of all sphingomyelin species detected were decreased and all but one ceramide species were increased in gp120tg mice compared with nTg mice. Chronic morphine had no effect on sphingomyelin or ceramide metabolism in nTg mice, but increased levels of several long chain sphingomyelins (C16:0-C22:0), and decreased levels of several long chain ceramides (C16:0-C20:0) in gp120tg mice. **c–d** There were no apparent alterations in sphingomyelin or ceramide metabolism during drug withdrawal in nTg mice. In gp120tg mice, brain levels of long chain sphingomyelin normalized (C16:0-C22:0), and levels of very long chain sphingomyleins were reduced (C24:0-C26:0), and all ceramide species were increased during drug withdrawal. ANOVA with Tukey post hoc comparisons (n=6 per group). *p<0.05, **p<0.01, ***p<0.001, ###p<0.001

Yang 2000; Brann et al. 1999; Ping and Barrett 1998; Inokuchi et al. 1998; Furuya et al. 1998; Furukawa and Mattson 1998; Ito and Horigome 1995). Disturbances in sphingolipid metabolism that result in the accumulations of ceramide have been associated with synaptic damage and activation of death pathways (see Haughey 2010 for a recent review)

We therefore quantified the postsynaptic marker PSD95 to determine if there were alterations in synaptic integrity associated with chronic morphine administration or morphine withdrawal. Chronic morphine administration decreased PSD95 levels by 63.0±10.4% in nTg mice (Fig. 4a), consistent with reports that morphine alone reduces neuronal spine density (Fitting et al. 2010). During morphine withdrawal in nTg mice, PSD95 levels rapidly recovered to levels comparable with nTg mice administered placebo (Fig. 4b). Chronic morphine administration in gp120tg mice resulted in a 42.8±8.1% decrease of PSD95 compared with gp120tg mice administered placebo (Fig. 4c). PSD95 did not recover during morphine withdrawal in gp120tg mice and remained decreased by 46.1±4.3% (Fig. 4d). These data demonstrate that morphine induced synaptic damage in both nTg and gp120tg mice, but that this neuronal damage rapidly recovered in nTg, but did not recover in gp120tg mice during the initial period of drug withdrawal.

Discussion

These findings highlight important differences in the neuronal response to morphine intoxication and drug withdrawal between nTg mice and gp120tg mice. In nTg mice, morphine intoxication increased oxidative stress in hippocampus without significantly altering sphingolipid metabolism, and induced neuronal damage that was evidenced by decreased synaptic integrity. These morphine-induced alterations in redox balance rapidly normalized in nTg mice during drug withdrawal and there were no apparent effects on sphingolipid

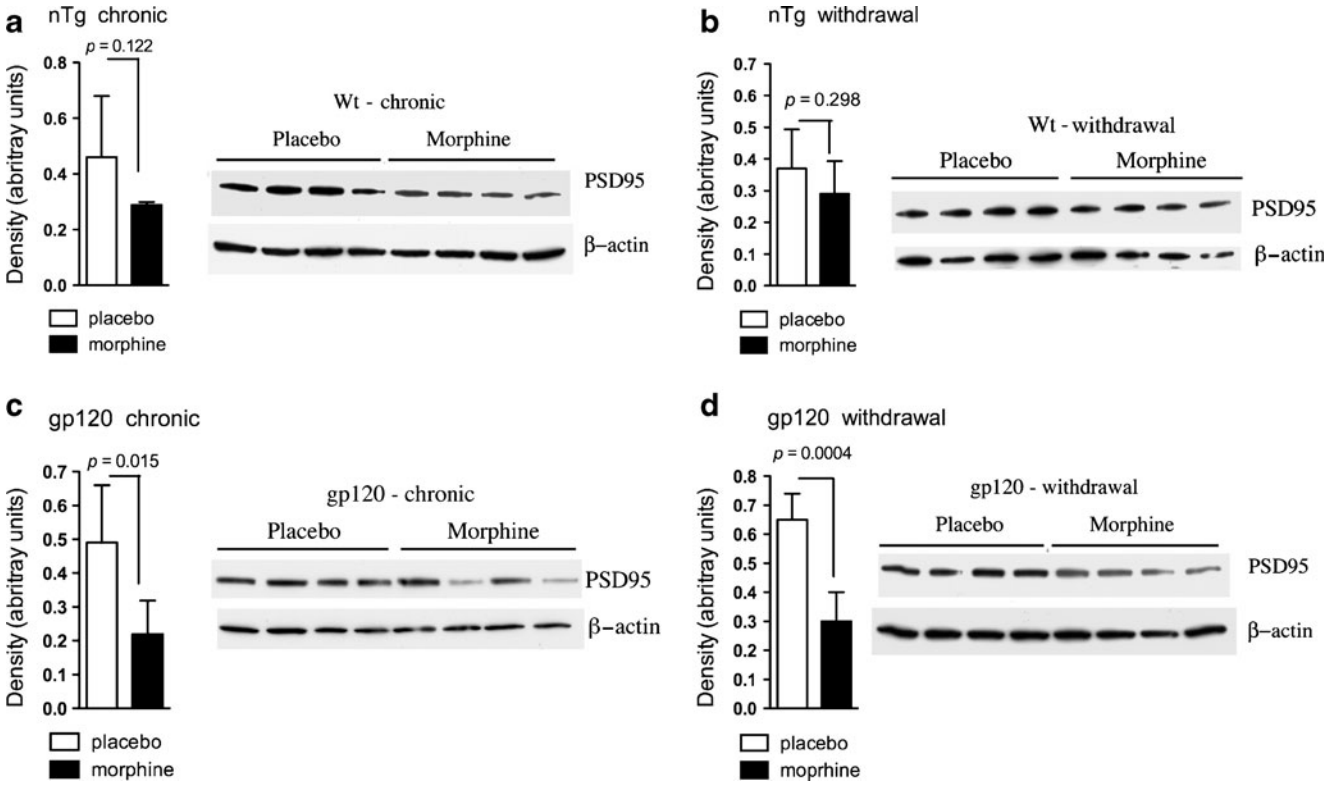

Fig. 4 Morphine-induced synaptic damage does not recover during drug withdrawal in gp120tg mice. **a**–**b** Levels of PSD95 in hippocampus were decreased in nTg mice during chronic morphine administration and recovered to levels similar to those measured in mice administered placebo. **c**–**d** Hippocampal levels of PSD95 were decreased in gp120tg mice during chronic morphine administration compared with placebo, and did not recover during drug withdrawal. For quantitative analysis, the densities of PSD95 were normalized to the corresponding β-actin density. Students *T*-test (n=4 per condition). Exact p values are shown

metabolism or synaptic integrity during drug withdrawal. In contrast, morphine intoxication in gp120tg mice increased oxidative stress, increased multiple species of sphingomyelin, decreased several species of ceramide, and induced synaptic damage. During drug withdrawal in gp120tg mice, oxidative stress did not normalize in (with the exception of uric acid levels), sphingomyelin levels normalized or were decreased (dependent on the species), ceramide was increased, and synaptic damage did not recover. These findings suggest that in addition to the combined effects of morphine and HIV proteins on glial and neuronal functions in the setting of acute and chronic drug use, there are additional effects during opiate withdrawal that have implications for the neuropathogenesis of HAND in subjects who abuse opiates.

The primary biochemical differences that we observed in nTg compared with gp120tg mice in response to chronic morphine were in sphingolipid metabolism. In gp120tg mice, there were baseline disruptions of spingolipid metabolism with reductions in sphingomyelin species and accumulations of long chain ceramides compared with nTg mice, suggesting that gp120 itself perturbed the pathways for sphingolipid metabolism by promoting the hydrolysis of sphingomyelin to ceramide. Indeed, gp120 has been shown to activate neutral sphingomyelinase, a hydrolase enzyme that is responsible for breaking down sphingomyelin to ceramide and phosphocholine (Jana and Pahan 2004; Haughey et al. 2004). These initial disruptions in sphingomyelin and ceramide metabolism appeared to sensitize these biochemical pathways to the effects of morphine, since sphingomyelin and ceramide levels responded to morphine in gp120tg, but not in nTg mice. In particular, chronic morphine increased long chain sphingomyelins and decreased all ceramide species measured in gp120tg mice, suggesting that a synthetic pathway became active, and ceramide was converted to sphingomyelin. In the pathway for sphingomyelin synthesis, a phosphocholine head group is transferred from phosphatidylcholine onto ceramide by a phosphatidylcholine transferase (also known as sphingomyelin synthase). Two sphingomyelin synthases designated as 1 and 2 (SMS1, SMS2) have been identified. Human SMS1 is localized to the Golgi, while SMS2 resides primarily at the plasma membrane (Takeuchi et al. 1995; Huitema et al. 2004; Khoury et al. 2007; Tafesse et al. 2007). Although it is not clear at this time why sphingomyelin synthesis becomes active during morphine intoxication in gp120tg but not in nTg mice, one possibility is that the perturbation of sphingolipid metabolism by gp120 sensitizes these pathways to the effects of morphine. For

example, gp120 is known to enhance the catabolism of sphingomyelin to ceramide by increasing the activity of sphingomyleinase (Jana and Pahan 2004; Haughey et al. 2004). Morphine may suppress this activity, thus allowing ceramide to be converted to sphingomyelin. In the setting of drug withdrawal, this inhibition would be removed, and sphingomyelinases could again become overactive, converting this enlarged pool of sphingomyelin to ceramide. Consistent with this notion, morphine tolerance has been shown to stimulate enzymatic activities of spinal cord serine palmitoyltransferase, ceramide synthase, and acid sphingomyelinase (enzymes involved in de novo and catabolic pathways of ceramide synthesis) leading to nitroxidative stress, increased formation of TNF-α, IL-β and IL-6. Inhibition of ceramide synthesis or pharmacological inhibitors of ceramide, and S1P attenuated ceramide production, nitroxidative stress, and neuroimmune activation.

A second notable difference in the neural response to morphine was the inability of gp120tg mice to normalize brain ROS during drug withdrawal compared with nTg mice. There is a great deal of experimental evidence which demonstrates that sustained ROS production is damaging to neurons, and increased oxidative stress contributes to neural damage in brains of HIV infected subjects (Boven et al. 1999; Turchan et al. 2003; Haughey et al. 2004). Tissue culture and animal models of HAND have repeatedly shown that the HIV-1 proteins gp120 and Tat induce oxidative stress and increase expression of pro-inflammatory cytokines, and that antioxidants protect neurons from the damaging effects of these neurotoxic HIV proteins (Mattson et al. 2005; Haughey and Mattson 2002; Turchan et al. 2003; Kruman et al. 1998). There are a number of interesting interactions between ROS and sphingolipid metabolism which suggest that ROS may play a significant role in driving the perturbation of sphingolipid metabolism and neuronal damage in the combined setting of gp120 and morphine. HIV-gp120 rapidly induces ceramide, then perturbs mitochondrial function and increase ROS over a period of hours (see Haughey et al. 2008 for a review), suggesting that an initial accumulation of the highly reactive intermediate ceramide may be a triggering event in gp120 -induced ROS. Indeed, synthetic cell-permeable ceramide analogs (C2-, C6- and C16-ceramides) rapidly perturb mitochondrial oxidative phosphorylation and induce cytochromoe C release by forming pores in the mitochondrial outer membrane that are permeable to molecules with a molecular mass less than 60,000. (Gudz et al. 1997; Ghafourifar et al. 1999; Siskind et al. 2002). ROS are known to have potent modulatory effects on sphingolipid metabolism. The activity sphingomyelinases (catalyzes the conversion of sphingomylelin to ceramide) are potently modulated by ROS that regulates location and function of these enzymes. For example, hydrogen peroxide (H_2O_2) induces trafficking of a neutral sphingomyelinase (nSMase) to the plasma membrane where it localizes into lipid raft domains, while the antioxidant glutathione, promotes the translocation and accumulation of nSMase in perinuclear regions (Levy et al. 2006). Likewise, peroxynitrate ($ONOO^-$) increases activity of an acidic sphingomyelinase (aSMase) and nitric oxide (NO) can protect cells from apoptotic death by inhibiting the activity of aSMase (Falcone et al. 2004; Castillo et al. 2007; Barsacchi et al. 2002). However, at high concentrations, NO can induce death by activating both nSMase and aSMase (Huwiler et al. 1999). Thus, the continued presence of ROS during drug withdrawal in gp120 transgenic mice may drive the increased generation of ceramide and impede the repair of synapses during drug withdrawal. Since these experiments were conducted during early stages of drug withdrawal, is not possible to conclude if these changes in sphingolipid metabolism, oxidative stress measures, or failure to repair synapses would recover over longer periods of time following drug cessation.

Sphingolipid metabolism is disrupted in the CNS of HIV-infected patients resulting in accumulations of multiple ceramide and sphingomyelin species. Moreover, the temporal progression of HAND can be predicted, and is associated with changes in sphingolipid metabolism (Sacktor et al. 2004; Cutler et al. 2004; Haughey et al. 2004; Mielke et al. 2010; Bandaru et al. 2007). Although, the potential interactions of drugs of abuse, and opiates in particular, on these biomarkers has not yet been addressed, our data suggest that here are likely to be complex interactions between opiates in the setting of HIV-infection that dysregulate sphingolipid metabolism and associated signaling pathways in both chronic and drug withdrawal conditions. In our model system morphine was introduced into a setting in which gp120 was actively being expressed. In humans, opiate abuse typically precedes HIV-infection. Our data would suggest that a failure to repair synapses would contribute to rapid declines of cognitive function that are apparent in opiate abusers who become infected with HIV. These combined findings suggest that opiate use may prime the CNS to damage that is induced during drug withdrawal in the setting of HIV infection.

Acknowledgments This work was supported by NIH grants AG034849, AA017408, MH077542.

Conflict of interest The authors have no conflicts of interest to report.

References

Bandaru VV, McArthur JC, Sacktor N, Cutler RG, Knapp EL, Mattson MP, Haughey NJ (2007) Associative and predictive biomarkers of dementia in HIV-1-infected patients. Neurology 68:1481–1487

Barsacchi R, Perrotta C, Sestili P, Cantoni O, Moncada S, Clementi E (2002) Cyclic GMP-dependent inhibition of acid sphingomyeli-

nase by nitric oxide: an early step in protection against apoptosis. Cell Death Differ 9:1248–1255

Beltran JA, Pallur A, Chang SL (2006) HIV-1 gp120 up-regulation of the mu opioid receptor in TPA-differentiated HL-60 cells. Int Immunopharmacol 6:1459–1467

Boven LA, Gomes L, Hery C, Gray F, Verhoef J, Portegies P, Tardieu M, Nottet HS (1999) Increased peroxynitrite activity in AIDS dementia complex: implications for the neuropathogenesis of HIV-1 infection. J Immunol 162:4319–4327

Brann AB, Scott R, Neuberger Y, Abulafia D, Boldin S, Fainzilber M, Futerman AH (1999) Ceramide signaling downstream of the p75 neurotrophin receptor mediates the effects of nerve growth factor on outgrowth of cultured hippocampal neurons. J Neurosci 19:8199–8206

Bruce-Keller AJ, Turchan-Cholewo J, Smart EJ et al (2008) Morphine causes rapid increases in glial activation and neuronal injury in the striatum of inducible HIV-1 Tat transgenic mice. Glia 56:1414–1427

Castillo SS, Levy M, Thaikoottathil JV, Goldkorn T (2007) Reactive nitrogen and oxygen species activate different sphingomyelinases to induce apoptosis in airway epithelial cells. Exp Cell Res 313:2680–2686

Chang SL, Beltran JA, Swarup S (2007) Expression of the mu opioid receptor in the human immunodeficiency virus type 1 transgenic rat model. J Virol 81:8406–8411

Cutler RG, Haughey NJ, Tammara A, McArthur JC, Nath A, Reid R, Vargas DL, Pardo CA, Mattson MP (2004) Dysregulation of sphingolipid and sterol metabolism by ApoE4 in HIV dementia. Neurology 63:626–630

El-Hage N, Gurwell JA, Singh IN, Knapp PE, Nath A, Hauser KF (2005) Synergistic increases in intracellular Ca2+, and the release of MCP-1, RANTES, and IL-6 by astrocytes treated with opiates and HIV-1 Tat. Glia 50:91–106

Emeterio EP, Tramullas M, Hurle MA (2006) Modulation of apoptosis in the mouse brain after morphine treatments and morphine withdrawal. J Neurosci Res 83:1352–1361

Falcone S, Perrotta C, De Palma C, Pisconti A, Sciorati C, Capobianco A, Rovere-Querini P, Manfredi AA, Clementi E (2004) Activation of acid sphingomyelinase and its inhibition by the nitric oxide/cyclic guanosine 3′,5′-monophosphate pathway: key events in Escherichia coli-elicited apoptosis of dendritic cells. J Immunol 173:4452–4463

Fitting S, Xu R, Bull C, Buch SK, El-Hage N, Nath A, Knapp PE, Hauser KF (2010) Interactive comorbidity between opioid drug abuse and HIV-1 Tat: chronic exposure augments spine loss and sublethal dendritic pathology in striatal neurons. Am J Pathol 177:1397–1410

Furukawa K, Mattson MP (1998) The transcription factor NF-kappaB mediates increases in calcium currents and decreases in NMDA- and AMPA/kainate-induced currents induced by tumor necrosis factor-alpha in hippocampal neurons. J Neurochem 70:1876–1886

Furuya S, Mitoma J, Makino A, Hirabayashi Y (1998) Ceramide and its interconvertible metabolite sphingosine function as indispensable lipid factors involved in survival and dendritic differentiation of cerebellar Purkinje cells. J Neurochem 71:366–377

Ghafourifar P, Klein SD, Schucht O, Schenk U, Pruschy M, Rocha S, Richter C (1999) Ceramide induces cytochrome c release from isolated mitochondria. Importance of mitochondrial redox state. J Biol Chem 274:6080–6084

Gudz TI, Tserng KY, Hoppel CL (1997) Direct inhibition of mitochondrial respiratory chain complex III by cell-permeable ceramide. J Biol Chem 272:24154–24158

Gurwell JA, Nath A, Sun Q, Zhang J, Martin KM, Chen Y, Hauser KF (2001) Synergistic neurotoxicity of opioids and human immunodeficiency virus-1 Tat protein in striatal neurons in vitro. Neuroscience 102:555–563

Haughey NJ (2010) Sphingolipids in neurodegeneration. Neuromolecular Med 12:301–305

Haughey NJ, Mattson MP (2002) Calcium dysregulation and neuronal apoptosis by the HIV-1 proteins Tat and gp120. J Acquir Immune Defic Syndr 31 Suppl 2:S55–S61

Haughey NJ, Cutler RG, Tamara A, McArthur JC, Vargas DL, Pardo CA, Turchan J, Nath A, Mattson MP (2004) Perturbation of sphingolipid metabolism and ceramide production in HIV-dementia. Ann Neurol 55:257–267

Haughey NJ, Steiner J, Nath A, McArthur JC, Sacktor N, Pardo C, Bandaru VV (2008) Converging roles for sphingolipids and cell stress in the progression of neuro-AIDS. Front Biosci 13:5120–5130

Hauser KF, Houdi AA, Turbek CS, Elde RP, Maxson W 3rd (2000) Opioids intrinsically inhibit the genesis of mouse cerebellar granule neuron precursors in vitro: differential impact of mu and delta receptor activation on proliferation and neurite elongation. Eur J Neurosci 12:1281–1293

Hauser KF, Hahn YK, Adjan VV, Zou S, Buch SK, Nath A, Bruce-Keller AJ, Knapp PE (2009) HIV-1 Tat and morphine have interactive effects on oligodendrocyte survival and morphology. Glia 57:194–206

Hu S, Sheng WS, Lokensgard JR, Peterson PK (2005) Morphine potentiates HIV-1 gp120-induced neuronal apoptosis. J Infect Dis 191:886–889

Huitema K, van den Dikkenberg J, Brouwers JF, Holthuis JC (2004) Identification of a family of animal sphingomyelin synthases. EMBO J 23:33–44

Huwiler A, Pfeilschifter J, van den Bosch H (1999) Nitric oxide donors induce stress signaling via ceramide formation in rat renal mesangial cells. J Biol Chem 274:7190–7195

Inokuchi J, Mizutani A, Jimbo M et al (1998) A synthetic ceramide analog (L-PDMP) up-regulates neuronal function. Ann N Y Acad Sci 845:219–224

Ito A, Horigome K (1995) Ceramide prevents neuronal programmed cell death induced by nerve growth factor deprivation. J Neurochem 65:463–466

Jana A, Pahan K (2004) Human immunodeficiency virus type 1 gp120 induces apoptosis in human primary neurons through redox-regulated activation of neutral sphingomyelinase. J Neurosci 24:9531–9540

Khoury CM, Yang Z, Ismail S, Greenwood MT (2007) Characterization of a novel alternatively spliced human transcript encoding an N-terminally truncated Vps24 protein that suppresses the effects of Bax in an ESCRT independent manner in yeast. Gene 391:233–241

Khurdayan VK, Buch S, El-Hage N et al (2004) Preferential vulnerability of astroglia and glial precursors to combined opioid and HIV-1 Tat exposure in vitro. Eur J Neurosci 19:3171–3182

Kruman I, Nath A, Mattson MP (1998) HIV protein Tat induces apoptosis by a mechanism involving mitochondrial calcium overload and caspase activation. Exp Neurol 154: 276–288

Levy M, Castillo SS, Goldkorn T (2006) nSMase2 activation and trafficking are modulated by oxidative stress to induce apoptosis. Biochem Biophys Res Commun 344:900–905

Liu WT, Han Y, Liu YP, Song AA, Barnes B, Song XJ (2010) Spinal matrix metalloproteinase-9 contributes to physical dependence on morphine in mice. J Neurosci 30:7613–7623

Mahajan SD, Schwartz SA, Shanahan TC, Chawda RP, Nair MP (2002) Morphine regulates gene expression of alpha- and beta-chemokines and their receptors on astroglial cells via the opioid mu receptor. J Immunol 169:3589–3599

Mahajan SD, Aalinkeel R, Sykes DE, Reynolds JL, Bindukumar B, Fernandez SF, Chawda R, Shanahan TC, Schwartz SA (2008) Tight junction regulation by morphine and HIV-1 tat

modulates blood-brain barrier permeability. J Clin Immunol 28:528–541

Mattson MP, Haughey NJ, Nath A (2005) Cell death in HIV dementia. Cell Death Differ 12(Suppl 1):893–904

Mielke MM, Bandaru VV, Haughey NJ, Rabins PV, Lyketsos CG, Carlson MC (2010) Serum sphingomyelins and ceramides are early predictors of memory impairment. Neurobiol Aging 31:17–24

Ping SE, Barrett GL (1998) Ceramide can induce cell death in sensory neurons, whereas ceramide analogues and sphingosine promote survival. J Neurosci Res 54:206–213

Pitcher J, Shimizu S, Burbassi S, Meucci O (2010) Disruption of neuronal CXCR4 function by opioids: preliminary evidence of ferritin heavy chain as a potential etiological agent in neuro-AIDS. J Neuroimmunol 224:66–71

Sacktor N, Haughey N, Cutler R, Tamara A, Turchan J, Pardo C, Vargas D, Nath A (2004) Novel markers of oxidative stress in actively progressive HIV dementia. J Neuroimmunol 157:176–184

Siskind LJ, Kolesnick RN, Colombini M (2002) Ceramide channels increase the permeability of the mitochondrial outer membrane to small proteins. J Biol Chem 277:26796–26803

Stefano GB, Salzet M, Bilfinger TV (1998a) Long-term exposure of human blood vessels to HIV gp120, morphine, and anandamide increases endothelial adhesion of monocytes: uncoupling of nitric oxide release. J Cardiovasc Pharmacol 31:862–868

Stefano GB, Salzet M, Rialas CM, Mattocks D, Fimiani C, Bilfinger TV (1998b) Macrophage behavior associated with acute and chronic exposure to HIV GP120, morphine and anandamide: endothelial implications. Int J Cardiol 64(Suppl 1):S3–S13

Sultana S, Li H, Puche A, Jones O, Bryant JL, Royal W (2010) Quantitation of parvalbumin+ neurons and human immunodeficiency virus type 1 (HIV-1) regulatory gene expression in the HIV-1 transgenic rat: effects of vitamin A deficiency and morphine. J Neurovirol 16:33–40

Tabatadze N, Savonenko A, Song H, Bandaru VV, Chu M, Haughey NJ (2010) Inhibition of neutral sphingomyelinase-2 perturbs brain sphingolipid balance and spatial memory in mice. J Neurosci Res 88:2940–2951

Tafesse FG, Huitema K, Hermansson M, van der Poel S, van den Dikkenberg J, Uphoff A, Somerharju P, Holthuis JC (2007) Both sphingomyelin synthases SMS1 and SMS2 are required for sphingomyelin homeostasis and growth in human HeLa cells. J Biol Chem 282:17537–17547

Takeuchi J, Okada M, Toh-e A, Kikuchi Y (1995) The SMS1 gene encoding a serine-rich transmembrane protein suppresses the temperature sensitivity of the htr1 disruptant in Saccharomyces cerevisiae. Biochim Biophys Acta 1260:94–96

Toggas SM, Masliah E, Rockenstein EM, Rall GF, Abraham CR, Mucke L (1994) Central nervous system damage produced by expression of the HIV-1 coat protein gp120 in transgenic mice. Nature 367:188–193

Turchan J, Pocernich CB, Gairola C et al (2003) Oxidative stress in HIV demented patients and protection ex vivo with novel antioxidants. Neurology 60:307–314

Turchan-Cholewo J, Dimayuga FO, Gupta S, Keller JN, Knapp PE, Hauser KF, Bruce-Keller AJ (2009) Morphine and HIV-Tat increase microglial-free radical production and oxidative stress: possible role in cytokine regulation. J Neurochem 108:202–215

Wheeler D, Knapp E, Bandaru VV, Wang Y, Knorr D, Poirier C, Mattson MP, Geiger JD, Haughey NJ (2009) Tumor necrosis factor-alpha-induced neutral sphingomyelinase-2 modulates synaptic plasticity by controlling the membrane insertion of NMDA receptors. J Neurochem 109:1237–1249

Yang SN (2000) Ceramide-induced sustained depression of synaptic currents mediated by ionotropic glutamate receptors in the hippocampus: an essential role of postsynaptic protein phosphatases. Neuroscience 96:253–258